DOI: https://doi.org/10.31351/vol32issSuppl.pp316-325

Preparation and Characterization of Vemurafenib Microemulsion[#]

Mohammed J. Neamah[*,1] and Entidhar J. Al-Akkam[1]

[#] 2nd Scientific Conference for Postgraduate Students Researches.

[1]Departure of Pharmaceutics, College of Pharmacy, University of Baghdad, Iraq.

Abstract

Human melanoma is the most common and malignant type of skin cancer. Vemurafenib has been used for the treatment of malignant or metastatic melanoma. Oral vemurafenib has serious adverse drug reactions including QTc segment (which is a part of heart ECG and their prolongation means a serious deterioration in heart function) prolongation of heart ECG which is the main reason for discontinuation of treatment with this drug. The study aimed to prepare oil in water vemurafenib microemulsion to be used for topical administration. Saturated solubility of vemurafenib was performed in different oils (peppermint, oleic acid, turpentine, cardamom, and orange oil), surfactants (Tween 20, Tween 60, and Tween 80), and co-surfactants (PEG-200, PEG-400, and 1-butanol). Peppermint oil, Tween 20, and PEG 400 were chosen to be the oil phase, surfactant, and co-surfactant respectively, since, vemurafenib had the highest solubility in these materials. Six formulas (F1- F6) of vemurafenib microemulsion were prepared by simple titration method and characterized for their particle size, polydispersity index (PDI), zeta potential, microemulsion morphology, dilution test, conductivity, thermodynamic stability, and drug release. Formula F3 (peppermint oil 10%, Tween 20 35%, and PEG 400 35%) was chosen since it exhibits the lowest particle size (11.83 nm ± 0.55 nm), zeta potential -2.57 mV, passed the thermodynamic stability tests and had significantly higher ($P < 0.05$) release percent for vemurafenib from the microemulsion particles (91% within 24 h). In conclusion, the microemulsion is considered a powerful and promising drug delivery system for topical administration.

Keywords: microemulsion, pepermint oil, pseudoternary phase diagram, saturated solubility, Vemurafenib.

تحضير وتوصيف المستحلب الدقيق لفيمورافينيب[#]

محمد جاسم نعمة *[،١] و انتظار جاسم العكام[١]

#المؤتمر العلمي الثاني لطلبة الدراسات العليا

[١]فرع الصيدلانيات ،كلية الصيدلة، جامعة بغداد، بغداد،العراق.

الخلاصة

مرض الميلانومة البشري هو أكثر أنواع سرطان الجلد شيوعًا وخبثاً. تم استخدام علاج الفيمورافينيب لعلاج الورم الميلانيني الخبيث أو المنتشر. الفيمورافينيب الفموي له اعراض جانبية خطيرة بما في ذلك إطالة QTc segment التي توضح في تخطيط القلب (ECG) والتي قد تؤدي إلى توقف استعمال العلاج. كان الهدف من الدراسة هو تحضير مستحلب دقيق يحتوي على الفيمورافينيب لاستخدامه في العلاج الموضعي لمرض الميلانومة على الجلد. تم إجراء فحص ذوبانية وتشبع الفيمورافينيب في زيوت مختلفة ، مواد خافضة للتوتر السطحي والمواد مساعدة للمواد الخافضة للتوتر السطحي. تم اختيار زيت النعناع ، Tween 20 و PEG 400 ليكون طور الزيت ، المادة الخافضة للتوتر السطحي والمادة مساعدة للمادة الخافضة للتوتر السطحي ذلك لان الفيمورافينيب تمتع بأعلى للذوبانية في تلك المواد. تم تحضير ستة من المستحلبات الدقيقة (F1- F6) التي تحتوي على الفيمورافينيب بطريقة الاضافة التدريجي للماء وتم اجراء فحوصات لمعرفة حجم جسيمات المستحلب الدقيق، تعدد احجام الجسيمات (PDI)، جهد زيتا او فرق الجهد بين الجسيمات ، اشكال او مورفولوجية جسيمات المستحلب الدقيق ، اختبار التخفيف ، التوصيل الكهربائي ، الاستقرار الديناميكي والحراري وسرعة خروج الدواء من المستحلب الدقيق. تم اختيار المستحلب الدقيق الحامل لصيغة F3 لأنه يحتوي على أقل حجم للجسيمات المستحلب الدقيق (١١,٨٣ نانومتر ± ٠,٥٥ نانومتر) ، جهد زيتا -٢,٥٧ ملي فولت ، اجتازت اختبارات الثبات الديناميكي والحراري وكانت نسبة إنطلاق او خروج الفيمورافينيب من المستحلب الدقيق أعلى بكثير (P <٠,٠٥) (91٪ خلال ٢٤ ساعة) مقارنتًا ببقية المستحلبات الدقيقة المحضرة. في الختام ، يعتبر المستحلب الدقيق نظامًا قويًا وواعدًا للإعطاء الموضعي للأدوية.

الكلمات المفتاحية: مستحلب دقيق، زيت النعناع، مخطط طور الشبه الثلاثي، الذوبانية والتشبع ، الفيمورافينيب.

Introduction

Vemurafenib (VRB) is propane-1-sulfonic acid {3-[5-(4-chlorophenyl)-1H-pyrrolo[2,3-b] pyridine-3-carbonyl]-2,4-difluoro-phenyl}-amide (Figure 1). It has the molecular formula $C_{23}H_{18}C_lF_2N_3O_3S$ and a molecular weight of 489.9 g/mol. VRB acts as a selective inhibitor of BRAF V600E kinase and it is recommended for the treatment of patients with metastatic or malignant melanoma who have been identified as having the BRAF V600E mutation by an FDA-approved test [(1)].

[1]Corresponding author E-mail: phmohammedneamah@gmail.com

Received: 6 / 5 /2023

Accepted: 16/10/2023

It has the molecular formula $C_{23}H_{18}ClF_2N_3O_3S$ and a molecular weight of 489.9 g/mol. VRB acts as a selective inhibitor of BRAF V600E kinase and it is recommended for the treatment of patients with metastatic or malignant melanoma who have been identified as having the BRAF V600E mutation by an FDA-approved test [(1)]. The stable and unstable crystalline forms of VRB have poor aqueous solubility (< 0.1 µg/ml), which leads to low bioavailability. Oral use of VRB has serious adverse drug reactions including QTc prolongation of heat ECG that results in reduction, temporary interruption, or discontinuation of treatment [(2)]. In addition, VRB is classified as a Class IV drug having aqueous buffer solubility (pH ranging from 3 to 7) of less than 0.1 µg/mL and estimated permeability of 0.0000029 cm/h which limits its oral absorption [(3)]

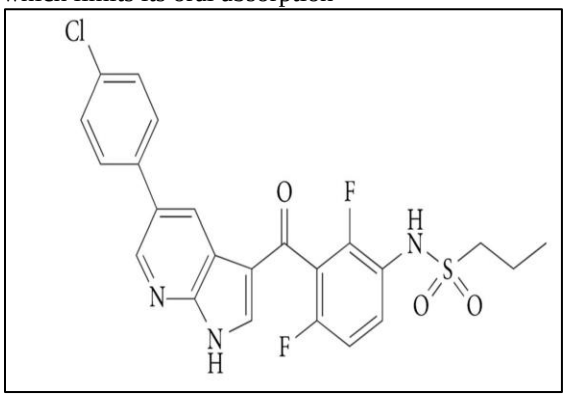

Figure 1 Structure of VRB [(2)].

Topical medications have been employed for the treatment of skin diseases as they are applied directly to the site of action and overcome the systemic use of drugs [(4)]. Microemulsion (ME) is considered a promising dosage form for topical delivery of drugs since it has a thermodynamically stable and transparent system in addition to the simple preparation method [(5)] [(6)]. ME is prepared from oils, surfactants, cosurfactants, and water with particle sizes of 5-100 nm [(7)]. ME can be classified into the water in oil (w/o), oil in water (o/w), and biocontinuous phase ME which can be affected by types of surfactant, co-surfactant, and the ratio of dispersed phase to dispersion media (oil to water ratio) [(8)].

Surfactants and co-surfactants play a crucial role in the formation of the ME system. Surfactants are adsorbed at the oil/water interface and can decrease oil/water interfacial tension resulting in the formation of ME droplets [(9)].

Co-surfactants have molecular lower than that of surfactants and usually have alcoholic or amine functional groups in their structure. The incorporation of co-surfactants in the ME system dramatically decreases the surface at the oil/water interface to ultralow values and increases the curvature of the ME system resulting in further decreasing ME droplet size [(10)]. Figure 2 shows the typical structure of o/w ME.

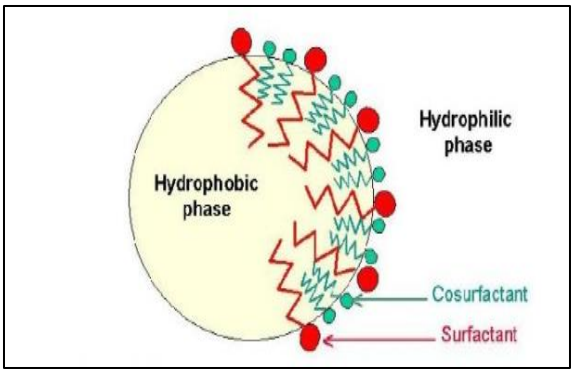

Figure 2. Typical structure o/w ME [(11)].

Surfactants and co-surfactants are used as penetration enhancers that disrupt the intact lipid layer of the stratum corneum [(12)]. The selection of the type and concentration of surfactant is crucial, since, some surfactants can cause skin irritation relative to melanoma. Non-ionic surfactants are commonly used because of their low toxicity and skin irritation effect [(13)].

There is several micro- and nanoemulsion marketed and intended for topical use on the skin. For example, Estrasorb® is an estradiol hemihydrate nanoemulsion composed of soybean oil, water, span 80, and ethanol and is used to manage vasomotor symptoms in menopausal women after application on the leg. the for application to the legs in the management of vasomotor symptoms associated with menopause. In the same point of view, Topicaine® is a microemulsion-based gel product for topical delivery of lidocaine and used for pain relief [(14)].

The study aimed to prepare VRB ME and then characterize them for their particle size, polydispersity index (PDI), zeta potential, ME morphology, dilution test, conductivity, thermodynamic stability, and drug release to be administered topically and replace the oral use of VRB and omitting the side effect and systemic toxicity of oral VRB.

Materials and Methods

Materials

VRB was purchased from Hangzhou Hyper Chemicals, China. Peppermint oil (BAR_SUR_LOUP, France), PEG 200 and PEG 400 (Vardaan House, India) Cardamom oil (Iraqi flavored company, Iraq), oil of turpentine (BDH chemical limited, England), orange oil (HENSTED TULBURG, Germany), Eucalyptus oil (Evans Medical, England) and Tween 20, Tween 60, Tween 80 (Avonchem, England), potassium dihydrogen phosphate, disodium

hydrogen phosphate, 1-butanol (Chem-Lab, Belgium) and hexadecyltriammonium bromide (HTAB) (Himedia, India).

Methods

Determination of saturated solubility of VRB

Saturated solubility was determined by adding an excess amount of VRB to 10 ml of each oil (peppermint, oleic acid, turpentine, cardamom, and orange oil), surfactants (Tween 20, Tween 60, and Tween 80) and co-surfactant (PEG-200, PEG-400, and 1-butanol) are placed in glass vials and sealed tightly. These vials are incubated for 72 h at 37 ± 1 °C in a shaker water bath. After that, the resultant mixtures were centrifuged at 6000 rpm for 10 minutes to separate the undissolved drugs and filtered using a 0.45 µm microfilter [15]. The dissolved drug in the supernatant layer was determined spectrophotometrically at 305 nm [16].

Construction of pseudo-ternary phase diagram

A pseudo ternary phase diagram was constructed by mixing different ratios of surfactant: co-surfactant (Smix) with different (1:1 and 1:2) peppermint oil and putting them in glass vials. The ratio of oil: Smix; 1:9, 2:8, 3:7, 4:6, 5:5, 6:4, 7:3, 8:2, and 9:1. Water was added to each vial drop by drop with continuous stirring at ambient temperature until turbidity appeared. The percent of different components of each vial was calculated and used to construct the pseudo ternary phase diagram using a ternary diagram generator (https://www.ternaryplot.com/) [17].

Microemulsion formulation

MEs were prepared by adding water to a mixture of VRB, oils, and surfactant/co-surfactant mixtures drop by drop with continuous stirring at 1500 rpm for 10 min. The clear translucent liquids were stored at room temperature to achieve equilibration [18]. Six formulas (F1-F6) were prepared and the quantity of each component in the formulas was presented in Table 1. Formulas F1, F2, and F3 had a Smix ratio of 1:1, and formulas F4, F5, and F6 had a Smix ratio of 1:2. Three different points, were selected from the o/w ME which are present in the pseudo ternary diagram, were used to prepare VRB ME. Formulas F1 and F4 are composed of peppermint oil 0.5 ml (10% of the formula), Smix 2.5 ml (50% of the formula), and water 2.0 ml (40% of the formula). Formulas F2 and F5 are composed of peppermint oil 0.5 ml (10% of the formula), Smix 3.0 ml (60% of the formula), and water 1.5 ml (30% of the formula). Formulas F3 and F6 are composed of peppermint oil 0.5 ml (10% of the formula), Smix 3.5 ml (70% of the formula), and water 1.0 ml (20 % of the formula).

Table 1. Composition of Different VRB ME.

Formula No.	*Percent of each ingredient*				*Smix ratio*	*Composition of different vemurafenib microemulsion*		
	Vemurafenib % w/v	*Peppermint oil % v/v*	*Smix % v/v*	*Water % v/v*		*Peppermint oil (mL)*	*Smix (mL)*	*Water (mL)*
F1	0.2	10	50	40	1:1	0.5	2.5	2.0
F2	0.2	10	60	30	1:1	0.5	3.0	1.5
F3	0.2	10	70	20	1:1	0.5	3.5	1.0
F4	0.2	10	50	40	1:2	0.5	2.5	2.0
F5	0.2	10	60	30	1:2	0.5	3.0	1.5
F6	0.2	10	70	20	1:2	0.5	3.5	1.0

Determination of particle size, polydispersity index (PDI), zeta potential

The ME was diluted to 10 ml with gentle mixing to preserve homogeneity. The particle size and PDI were measured by using a zeta sizer apparatus (Malvern, UK) [19] [20]. All formulas (F1-F6) were measured for their particle size. Zeta potential was measured for the selected formula only.

Determination of visual transparency and dilution test

The inspection of visual transparency was determined by visual inspection of ME whether it was translucent or not. A dilution test was performed by adding water to determine whether the dilution affected their transparency and to ensure the absence of turbidity in addition it gave an idea of whether the emulsion was o/w or w/o [21].

Electrical conductivity of VRB ME

Electrical conductivity was measured by using conductometer apparatus (TDS Ec Meter Temperature Tester, China). The probe of the conductometer was placed in 10 ml of each ME (F1-F6) formulation at room temperature and the resultant electrical current was measured by µs/cm [22].

Physical stability of ME

Thermodynamic stability of VRB ME (F1-F6) was performed by visual inspection of ME after

performing centrifugation and heating-cooling cycles. All ME were centrifuged at 3500 rpm for 30 min at 25 °C. While, the Heating-cooling cycle test was performed by storing MEs at 4 °C, then at 25 °C, and then at 40 °C for not less than 48 h for each temperature. After that, MEs were visualized for any separation or turbidity that indicated thermal instability [23] [24]. Formulas investigated all the stability studies were passed for further study (drug release).

Drug release

In-vitro release was performed using the dialysis bag method. A dialysis bag with 8000-14000 Dalton pore size was allowed to be hydrated in a solution of 1% hexadecyltriammonium bromide (HTAB) in 0.05 M phosphate buffer, pH 6.8 (the same dissolution media of VRB). One ml of VRB ME, which contained 2 mg VRB, was placed in a hydrated dialysis bag and sealed from the two sides. The dialysis bag is placed in 100 mL dissolution media rotated at 50 rpm at 37 °C. Sampling time would be 1 h, 2 h, 4 h, 6 h, 12 h, and 24 h from starting the experiment. The concentration of VRB was measured spectrophotometrically at 307 nm [25]. The percent of VRB was determined after applying the calibration curve equation.

Determination of VRB ME morphology by transmission electron microscopy (TEM)

For TEM examination, a clean petri dish with a copper grid hexagonal mesh was attached to carbon tape, and a liquid sample was placed on the grid and left for a short time before being loaded onto the TEM holder to be imaged with a scanning transmission electron microscopy (STEM) detector [26].

Fourier transform infrared (FTIR) analysis

Fourier transform infrared (FTIR) spectrum was performed by blending the pure drug with potassium bromide placing it in the sample holder and recording the FTIR absorption spectrum for the pure drug using FTIR (Shimadzu, Japan). The selected liquid formula was placed directly and the IR spectrum of it using the same device [27].

Statistical Analysis

Statistical analysis for all experimental data was performed using IBM SPSS statistic 25 software. Data were expressed as mean values with their standard deviation (SD). ANOVA with post hoc test was used to approve the significance between results with the level of significance ($P < 0.05$). DDsolver program was applied to detect the kinetic of drug release.

Results and Discussion

Determination of saturated solubility of VRB:

Solubility of VRB was found to be significantly higher in peppermint oil ($P < 0.05$) as compared with other oils as shown in Table 2. The solubility of VRB is better in molecules that have more amphiphilic properties. So, VRB had better solubility in Tween 20 than in Tween 80. In addition, VRB solubility in PEG 400 was significantly higher ($P < 0.05$) than that in PEG 200 and this observation may be attributed to the higher amphiphilic nature of PEG 400 and higher (-OH) groups present in PEG 400 structure when compared PEG 200 that may increase possibility of interaction with VRB functional groups with (-OH) in PEG 400 thereby increase its solubility in PEG 400 [28].

Table 2. Saturated Solubility of VRB in Different Oils, Surfactant and Co-surfactant.

	Compounds	VRB solubility (mg/ml)
Oils	Peppermint oil	17.6900± 0.35791
	Turpentine oil	3.0867± 0.07638
	Cardamom oil	0.5567± 0.02517
	Oleic acid	0.1767± 0.00577
	Orange oil	0.1533± 0.01528
Surfactant	Tween 20	15.7100± 0.44844
	Tween 80	10.3467± 0.12342
Co-surfactant	PEG 400	22.8533± 0.45633
	PEG 200	20.9067± 0.45281
	1-butanol	0.4687± 0.03859

(Results expressed as mean ± STD, n=3)

VRB has 2 lambdas max (305 nm and 252 nm, as shown in Figure 3 A) and the calibration curve was done for VRB at these 2 wavelengths. In the saturated solubility study, interference of UV spectrum of VRB with UV spectrum of additives was avoided by adding the same quantity of additives with methanol in the blank solution (for example, if I take 200 µL from peppermint oil that contains VRB and dilute it up to 10 ml, the blank solution would be 200 µL of pure peppermint oil and diluted up to 10 ml and measured for each lambda max and gave the same results.

But when the peppermint oil, Tween 200, and PEG 400 were chosen for ME preparation and used UV spectrum for content uniformity or release study, the UV spectrum for this ingredient and these additives forced to use lambda max 305 since they have a strong absorption at 252 nm that may interfere with results and figure 3 B below shows the absorption spectrum of peppermint oil.

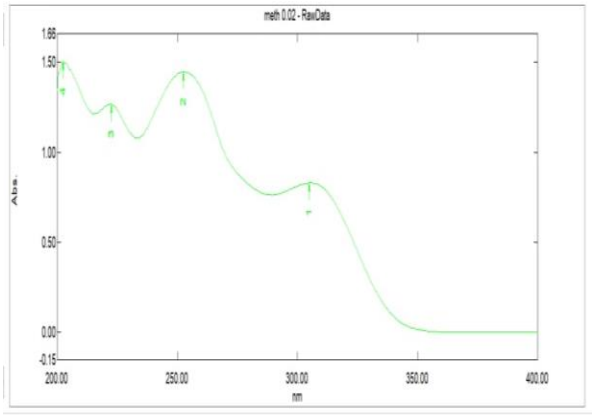

Figure 3 A

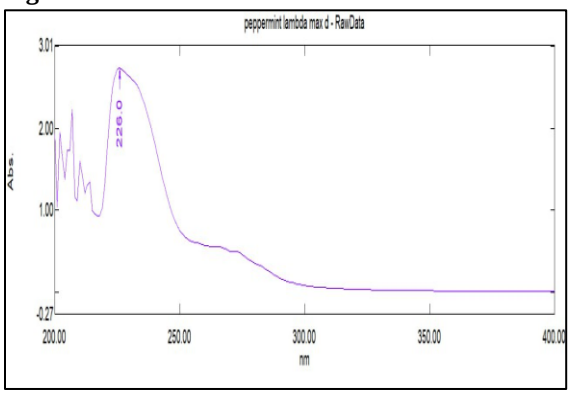

Figure 3 B

Figure 3. UV-spectrum of VRB and peppermint oil, surfactant. Figure 3 A represents the UV spectrum of VRB. Figure 3 A represents the UV spectrum of peppermint oil.

Construction of pseudo-ternary phase diagram

Figure 4 A represents the pseudoternary phase diagram when the Smix was 1:1 and Figure 4 B when the Smix ratio was 1:2. The dark area represents the coarse macroemulsion area and the white area represents the ME region.

Smix ratio 1:1, which had a higher quantity of Tween 20 and higher HLB value than Smix ratio 1:2, had a narrower microemulsion area (dark area) and higher ME area (white area). These results match the fact that the macroemulsion region tends to narrow down with increasing the ratio of surfactant to co-surfactant and higher HLB value of the system [29] [30]. So, an S mix ratio of 1:1 was better to be used to prepare VRB ME.

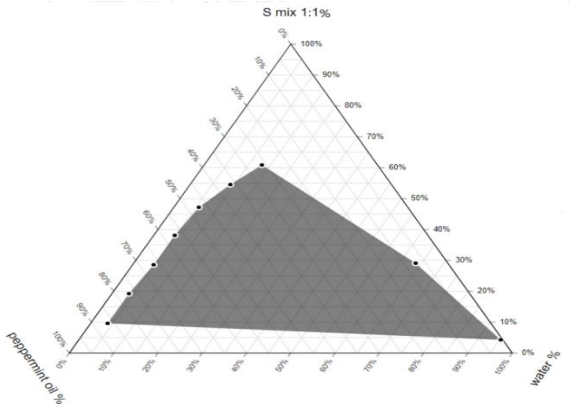

Figure 4 A

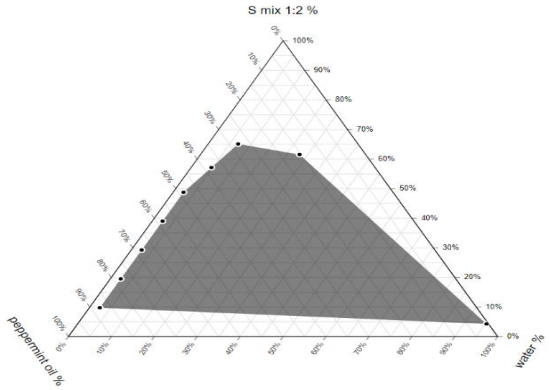

Figure 4 A

Figure 4. The pseudoternary phase diagram for the oil phase is peppermint oil, the surfactant is Tween 20 and the co-surfactant is PEG 400. Figure 4 A represents the pseudo ternary phase diagram for the Smix ratio 1:1. Figure 4 A represents the pseudo ternary phase diagram Smix ratio 1:2.

Particle size, polydispersity index (PDI), and zeta potential

The particle size of VRB microemulsion was measured by zeta sizer on the principle of dynamic light scattering (DLS) that measures the scattering of light resulting from the movement of particles by Brownian motion. ME samples were diluted before measuring the DLS to reserve the free movement of ME particles by Brownian motion.

The particle size of ME in formulas containing Smix ratio 1:1 which is present in formulas F1, F2, and F3 was 22.73± 0.67 nm, 17.67± 0.47 nm, and 11.83± 0.55 nm, respectively. While, the particle size formulas contain Smix 1:2, which is present in formulas F4, F5, and F6, was to 56.24± 2.14 nm, 45.70± 2.52 nm, and 36.37± 2.15 nm. The particle size was uniformly distributed as shown in Figure 5.

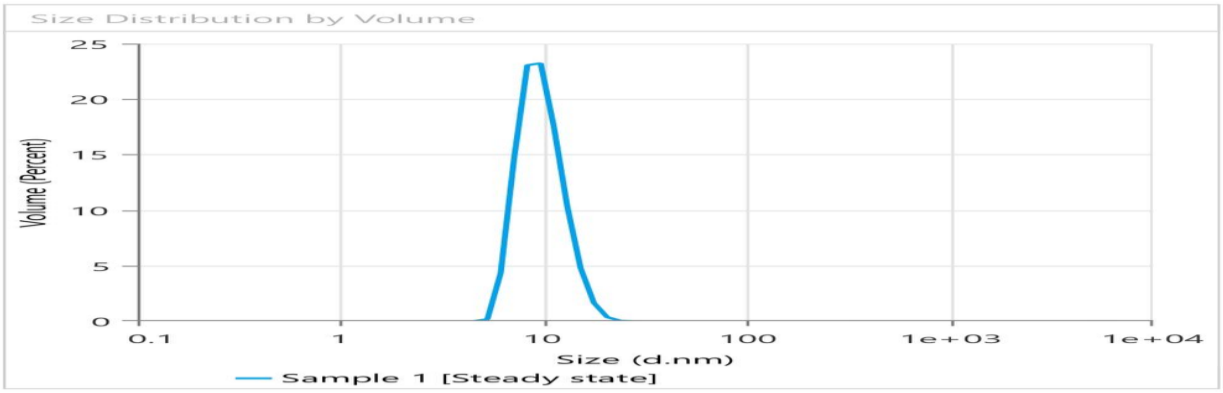

Figure 5. The plot of size distribution (per volume) for Formula F3

The results showed that increasing the concentration or percent of Smix against peppermint oil in the formulas, for the same Smix ratio, resulted in decreasing the particle size of ME. These outcomes can be explained by increasing the Smix concentration against oil would dramatically decrease the interfacial tension and break down the peppermint oil into smaller particle sizes [31].

The particle size of the formula with Smix 1:1 (F1-F3), which had a higher HLB value, was smaller than the particle size of the formula with Smix 1:2 (F4- F6), which had a lower HLB value. For example, the particle size of formula F1 was significantly smaller than that of formula F4 (even though both formulas had a Smix concentration of 50% but they differed in Smix ratio). The same results were found when comparing the particle size of formula F2 and that of formula F5 and the particle size of formula F3 and that of formula F6 and this observation may be attributed to the high emulsifying capacity found in formulas that had high HLB value [32]. Table 3 shows the mean particle size and mean PdI for the six prepared formulas.

The Zeta potential of the selected formula was -2.57 mV. The presence of non-ionic surfactants like Tween 20 results in low zeta potential since there is a sudden expulsion of the (-OH) group in Tween 20 at the o/w when the concentration of surfactants reaches CMC [33].

Table 3. The Mean Particle Size and Mean PdI for The Six Prepared Formulas.

Formula NO.	Particle size (nm)	Mean PdI
F1	22.73± 0.67	0.390± 0.0458
F2	17.67± 0.47	0.333± 0.0208
F3	11.83± 0.55	0.173± 0.0351
F4	56.24± 2.14	0.277± 0.0351
F5	45.70± 2.52	0.277± 0.0152
F6	36.37± 2.15	0.290± 0.0721

(Results expressed as mean ± STD, n=3)

Visual transparency and dilution test of VRB

All formulas are translucent and no turbidity was observed when diluted with distilled water which gave a good indication that VRB ME type is o/w.

Electrical conductivity of ME

An electrical conductivity test was performed to detect whether the prepared MEs were o/w or w/o. electrical current would be detected when the ME is o/w since water is the external phase.

The prepared VRB microemulsion had an electrical current between 10 to 15 µs/cm. the presence of an electrical current revealed that the prepared microemulsion was o/w. MEs with electrical conductivity between 10-100 µs/cm are considered o/w ME [34].

Formulas F1 and F4 had significantly higher (P < 0.05) electrical conductivity as compared with F3 and F6 which can be explained by the higher water content in these formulas compared with formulas F3 and F6[35]. Table 4 shows the mean electrical current of each formula in µs/cm.

Table 4. Mean Electrical Current of Each Formula in µs/cm.

Formula No.	Mean electrical current (µs/cm)
F1	13.3± 0.6
F2	12.7± 0.6
F3	10.3± 0.6
F4	12.7± 0.6
F5	12.3± 0.6
F6	10.6± 0.6

(Results expressed as mean ± STD, n=3)

Physical stability of ME

All formulas (F1-F6) passed the centrifugation test with no separation observed. Formulations F1, F2, and F4 showed turbidity and phase separation when stored at 4 ºC. Formulas F3, F5, and F6 passed all the stress conditions including centrifugation and storage at different temperatures (Table 5). So, F3, F5, and F6 were used for further characterization (drug release).

Table 5. shows the of putting different formulas in different stress conditions.

Formula No.	Physical stability observation			
	Centrifugation	4 °C	25 °C	40 °C
F1	Passed	Failed	Failed	Failed
F2	Passed	Failed	Passed	Passed
F3	Passed	Passed	Passed	Passed
F4	Passed	Failed	Failed	Failed
F5	Passed	Passed	Passed	Passed
F6	Passed	Passed	Passed	Passed

Drug release

The release profile of VRB of formulas F3, F5, and F6 are shown in Figure 6. Formula F3, which has a mean particle size of 11.8 ± 0.56 nm, showed a better release profile as compared with formulas F5 and F6. The percent of drug release VRB from formula F3 was approximately 91% after 24 h which was significantly higher ($P < 0.05$) than that of formula F5 (approximately 30%) and F6 (approximately 47%). The superior release of VRB from formula F3 can be attributed to the smaller particle size of ME in this formula since the tendency of drug release is increased as the particle size of the nanoparticle decreases [36]. The release profile kinetic of VRB from VRB microemulsion in formula F3 was analyzed using the DDsolver program. Table 6 shows the rate and R-squared (R^2) for different order kinetic for VRB from VRB microemulsion of formula F3. The results revealed that VRB release from ME followed a first-order reaction with R^2 equal to 0.96.

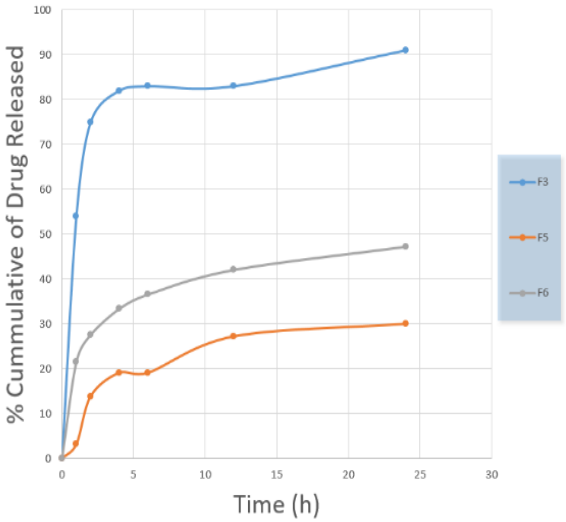

Figure 6. Release Profile of VRB from VRB Microemulsion formulas F3, F5, and F6.

Table 6. The Rate and R^2 for Different Order Kinetic for VRB from ME Formula F3.

Order	Zero order		First order		Higuchi		Korsymer-Peppas		
	K_0	R^2	K_1	R^2	K_H	R^2	N	K_{KP}	R^2
F3	5.418	0.69	0.639	0.96	25.7	0.79	0.12	64	0.87

VRB microemulsion morphology

The shape of the VRB microemulsion is shown in Figure 7. The ME particles were uniformly dispersed and didn't show any flocculation.

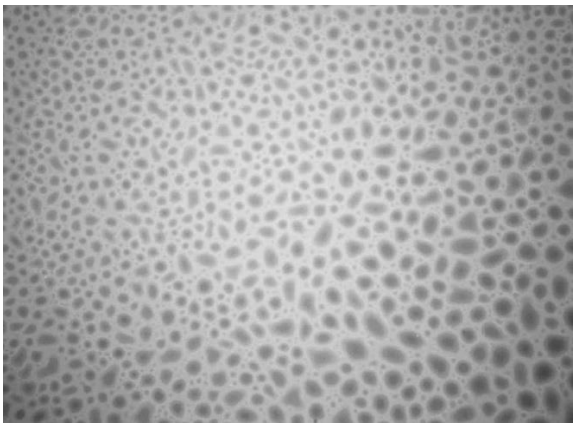

Figure 7. TEM Spectrum of VRB Microemulsion Formulas F3.

Fourier transform infrared (FTIR) analysis

FTIR analysis was performed to approve the compatibility of other ingredients in the selected formula (F3) with the drug and to confirm that the preparation condition didn't affect VRB stability.

Figure 8 A represents the FTIR absorption spectrum for the pure drug. Absorption bands at 3264 and 3116 cm^{-1} could be due to stretching vibrations of the ammonia N-H group. Absorption bands at 2966 and 2877 cm^{-1} could be due to stretching vibrations of the aliphatic C-H group. Absorption bands at 1735 cm^{-1} could be due to stretching vibrations of the ketone C=O group. Absorption bands at 1640 cm^{-1} could be due to stretching vibrations of the aromatic double bonds. Absorption bands at 1319 and 1141 cm^{-1} could be due to stretching vibrations of the SO_2 group.

Figure 8 B represents the FTIR absorption spectrum of the selected formula and shows a comparable absorption band with small shifts that represent the compatibility of VRB with other formula ingredients in the selected formula (F3).

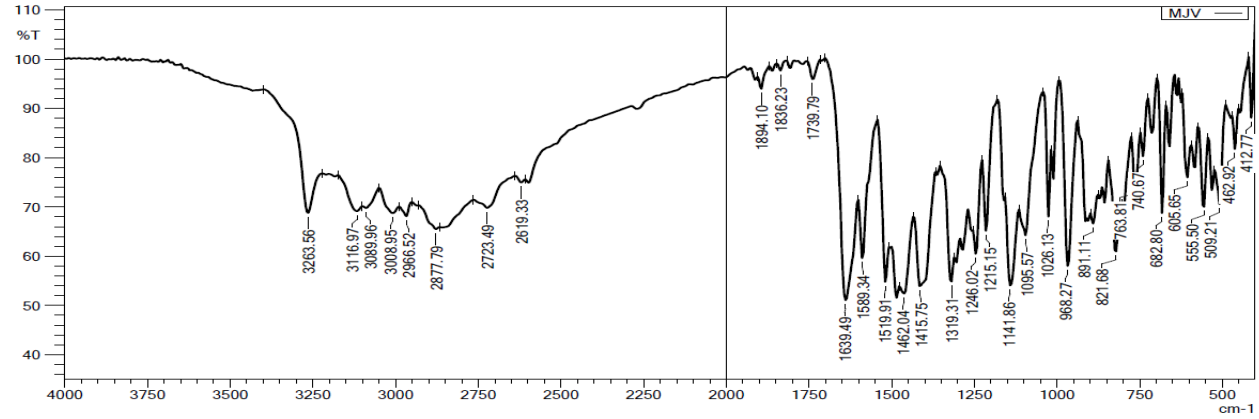

A

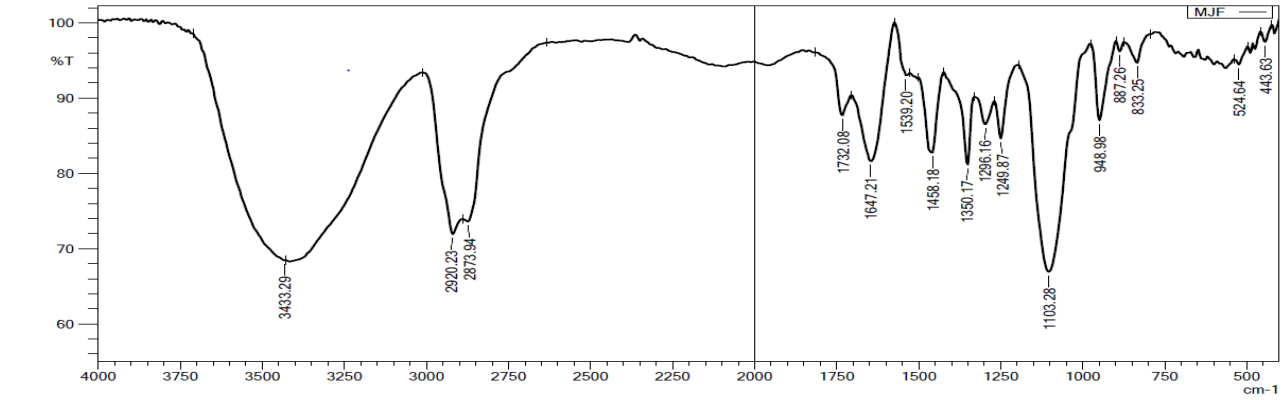

B

Figure 8. FTIR absorption spectrum of pure VRB and selected formula (F3). Figure 8 A represents the FTIR absorption spectrum of pure VRB. Figure 8 B represents the FTIR absorption spectrum of the selected formula (F3).

Conclusion

ME is considered a powerful and promising drug delivery system for VRB which may applied for topical administration. Formula F3, which is composed of 10 mg vemurafenib, 0.5 ml peppermint oil, 3.5 ml Smix (1:1), and 1 ml water, was selected as the best formula. It exhibits the lowest particle size (11.8 nm ± 0.55 nm), passed the thermodynamic stability tests, and had significantly higher ($P < 0.05$) release percent for VRB (91% within 24 h). As a future work, the prepared VRB microemulsion can be used for further study like permeation tests and ex-vivo cytotoxicity studies to elicit its feasibility for topical treatment of skin melanoma.

Acknowledgment

The authors thank the College of Pharmacy - University of Baghdad for their support and for providing the necessary facilities to complete this research.

Conflicts of Interest

The authors stated no conflict of interest in the manuscript.

Funding

non

Ethics Statements

There were no humans or animals used in all experiments

Author Contribution

The authors confirm their contribution to the paper as follows: study conception and design: Mohammed J Neamah has done all experiments and Entidhar J Al-Akkam made a valuable effort in the interpretation of data resulting from the characterization of prepared formulas. All authors reviewed the results and approved the final version of the manuscript.

References

1. Bollag G, Tsai J, Zhang J, Zhang C, Ibrahim P, Nolop K, & Hirth P. Vemurafenib: the first drug approved for BRAF-mutant cancer. Nature reviews Drug discovery. 2012;11(11): 873-886.

2. Ellenberger DJ, Miller DA, Kucera SU, et al. Improved vemurafenib dissolution and pharmacokinetics as an amorphous solid dispersion produced by KinetiSol® processing. AAPS PharmSciTech. 2018;19(5): 1957-1970.

3. Zhang W, Heinzmann D, Grippo JF. Clinical pharmacokinetics of vemurafenib. Clinical pharmacokinetics. 2017;56:1033-43.

4. Yamaguchi K, Mitsui T, Aso Y, & Sugibayashi K. Structure–permeability relationship analysis of the permeation barrier properties of the stratum corneum and viable epidermis/dermis of rat skin. Journal of Pharmaceutical Sciences, 2008; 97(10), 4391-4403.

5. Ngawhirunpat T, Worachun N, Opanasopit P, Rojanarata T, & Panomsuk S. Cremophor RH40-PEG 400 microemulsions as transdermal drug delivery carrier for ketoprofen. Pharmaceutical development and technology, 2013;18(4), 798-803.

6. Al-Rubaye RA & Al-Kinani KK. Formulation and Evaluation of Prednisolone Acetate Microemulsion Ocular Gel. *The Egyptian Journal of Hospital Medicine*. 2023;*90*(1):1744-1751.

7. Yang J, Xu H, Wu S, Ju B, Zhu D, Yan Y and et al. Preparation and evaluation of microemulsion-based transdermal delivery of Cistanche tubulosa phenylethanoid glycosides. Molecular Medicine Reports, 2017;15(3), 1109-1116.

8. Moulik SP, Rakshit AK. Physicochemistry and applications of microemulsions. Journal of Surface Science and Technology. 2006;22(3–4):159–186.

9. Artiga-Artigas M, Acevedo-Fani A & Martín-Belloso O. Effect of sodium alginate incorporation procedure on the physicochemical properties of nanoemulsions. *Food Hydrocolloids*. 2017;*70*: 191-200.

10. Smail, SS, Ghareeb MM, Omer HK, Al-Kinani AA & Alany RG. Studies on surfactants, cosurfactants, and oils for prospective use in formulation of ketorolac tromethamine ophthalmic nanoemulsions. *Pharmaceutics*. 2021;*13*(4): 467.

11. Srikanth, K, Gupta VR M, Manvi SR, & Devanna N. INTERNATIONAL RESEARCH JOURNAL OF PHARMACY. *2012; 3 (11):22-26.*

12. Kreilgaard M. Influence of microemulsions on cutaneous drug delivery. Advanced drug delivery reviews. 2002;54: S77-S98.

13. Taher SS, Al-Kinani KK, Hammoudi ZM, Ghareeb MM. Co-surfactant effect of polyethylene glycol 400 on microemulsion using BCS class II model drug. J Adv Pharm Educ Res. 2022;12(1):63-9.

14. Nastiti, CM, Ponto T, Abd E, Grice JE, Benson HA & Roberts MS. Topical nano and microemulsions for skin delivery. *Pharmaceutics*. 2017;*9*(4): 37.

15. Juškaitė V, Ramanauskienė K & Briedis V. Design and formulation of optimized microemulsions for dermal delivery of resveratrol. Evidence-Based Complementary and Alternative Medicine, 2015.

16. Morlière P, Boscá F, Silva A M S, Teixeira A, Galmiche A, Mazière JC, et al. A molecular insight into the phototoxic reactions observed

with vemurafenib, a first-line drug against metastatic melanoma. Photochemical & Photobiological Sciences2015;14: 2119-2127.

17. Anil L, & Kannan K. Microemulsion as drug delivery system for Peptides and Proteins. Journal of Pharmaceutical Sciences and Research. 2018;10(1):16-25.

18. Boonme P, Krauel K, Graf A, Rades T, & Junyaprasert V B. Characterization of microemulsion structures in the pseudoternary phase diagram of isopropyl palmitate/water/Brij 97: 1-butanol. Aaps Pharmscitech2006; 7: E99-E104.

19. Bayindir ZS and Yuksel N. Characterization of niosomes prepared with various nonionic surfactants for paclitaxel oral delivery. Pharmaceutical technology. 2010;99(4):2049-2060.

20. Basheer HS, Noordin MI, & Ghareeb MM . Characterization of microemulsions prepared using isopropyl palmitate with various surfactants and cosurfactants. *Tropical Journal of Pharmaceutical Research*. 2013;*12*(3), 305-310.

21. Nirmala MJ, Allanki SRI N IV A S, Mukherjee, A. M. I. T. A. V. A., & Chandrasekaran N. Enhancing the solubility of ramipril using a new essential oil based microemulsion system. Int J Pharm Pharm Sci. 2013;5(4):322-323.

22. Kalra R. Development and characterization of nanoemulsion formulations for transdermal Delivery of aceclofenac: A Research. Int. J. of drug formulation & Res. 2010; 1(1):359-86.

23. Thakkar PJ, Madan P, & Lin S. Transdermal delivery of diclofenac using water-in-oil microemulsion: formulation and mechanistic approach of drug skin permeation. Pharmaceutical development and technology. 2014;19(3):373-384.

24. Sadoon NA, and Ghareeb MM. Formulation and characterization of isradipine as oral nanoemulsion. *Iraqi Journal of Pharmaceutical Sciences.2020; 29*(1):143-153.

25. Dawood NM, Abdal-Hamid SN. Formulation and characterization of lafutidine nanosuspension for oral drug delivery system. Int J App Pharm 2018;10 Suppl 2:20-30.

26. Bansal S, Aggarwal G, Chandel P and Hirikumar SL.Design and development of cefdinir niosomes for oral delivery. Journal of pharmaceutical bioallied science. 2013;5(4):318-325.

27. Ali SK, Al-khedairy EBH. Solubility and Dissolution Enhancement of Atorvastatin Calcium using Solid Dispersion Adsorbate Technique. Iraqi J Pharm Sci. 2019;28(2):105–114.

28. Bergonzi MC, Hamdouch R, Mazzacuva F, Isacchi B, & Bilia AR. Optimization, characterization, and in vitro evaluation of curcumin microemulsions. LWT-Food Science and Technology. 2014;59(1):148-155.

29. Huang YB, Lin YH, Lu TM, Wang RJ, Tsai YH, Wu PC. Transdermal delivery of capsaicin derivative-sodium nonivamide acetate using microemulsions as vehicles. Int J Pharm 2008; 349:206–211.

30. Hammodi ID & Abd Alhammid SN. Preparation and Characterization of Topical Letrozole Nanoemulsion for Breast Cancer. *Iraqi Journal of Pharmaceutical Sciences.* 2020; *29*(1):195-206.

31. Hamed SB, & Abd Alhammid SN. Formulation and Characterization of Felodipine as an Oral Nanoemulsions. *Iraqi Journal of Pharmaceutical Sciences.* 2021;*30*(1) :209-217.

32. Krstić M, Medarević Đ, Đuriš J, & Ibrić. Self-nanoemulsifying drug delivery systems (SNEDDS) and self-microemulsifying drug delivery systems (SMEDDS) as lipid nanocarriers for improving dissolution rate and bioavailability of poorly soluble drugs. In Lipid nanocarriers for drug targeting 2018:473-508.

33. Manev ED & Pugh RJ. Diffuse layer electrostatic potential and stability of thin aqueous films containing a nonionic surfactant. *Langmuir*. 1991;*7*(10): 2253-2260.

34. Park ES, Cui Y, Yun BJ, Ko IJ, & Chi SC. Transdermal delivery of piroxicam using microemulsions. Archives of pharmacal research. 2005; 28: 243-248.

35. Baroli B, López-Quintela MA, Delgado-Charro MB, Fadda, AM, & Blanco-Méndez J. Microemulsions for topical delivery of 8-methoxsalen. Journal of Controlled Release. 2000;69(1):209-218.

36. Sun J, Wang F, Sui Y, She Z, Zhai W, Wang C, & Deng Y. Effect of particle size on solubility, dissolution rate, and oral bioavailability: evaluation using coenzyme Q10 as naked nanocrystals. International journal of nanomedicine. 2012;5733-5744.